International Journal of Thermophysics, Vol. 6, No. 5, 1985

Aluminum. II. Derivation of C_{v0} from C_p and Comparison to C_{v0} Calculated from Anharmonic Models

R. C. Shukla,[1] C. A. Plint,[1] and D. A. Ditmars[2]

Received May 3, 1985

The specific heat at constant pressure, C_p, of aluminum measured by Ditmars, Plint, and Shukla has been reduced to the volume V_0 appropriate for 0 K employing the Murnaghan equation. The C_{v0} thus obtained is compared with the theoretical C_{v0} calculated in the harmonic and the lowest-order anharmonic approximation from three different pseudopotentials (Harrison, Ashcroft, and Dagens–Rasolt–Taylor) as well as a phenomenological Morse potential. The higher-order (λ^4) anharmonic contributions are calculated from the same nearest-neighbor Morse potential as in the lowest-order anharmonic theory. The role of the vacancy and the higher-order anharmonic contributions to C_{v0} has been examined and we conclude that the λ^4 contributions to C_{v0} are much smaller than the vacancy contribution. After removal of the vacancy contribution, the reduced C_{v0} is found to be in excellent agreement with the Ashcroft and Harrison pseudopotentials as well as the Morse potential including the λ^2 and λ^4 contributions to C_{v0}.

KEY WORDS: aluminum; Helmholtz free energy; anharmonic Al fcc crystal; constant-volume specific heat; heat capacity; interionic potentials for Al; perturbation theory to $O(\lambda^2)$ and $O(\lambda^4)$; Van Hove order parameter (λ).

1. INTRODUCTION

Ample justification for a definitive measurement of the specific heat at constant pressure (C_p) of Al in the temperature range 273 to 933 K came from the recent work of Shukla and Plint [1]. The preceding paper [2] presents

[1] Physics Department, Brock University, St. Catharines, Ontario L2S 3Al, Canada.
[2] Chemical Thermodynamics Division, National Bureau of Standards, Gaithersburg, Maryland 20899, U.S.A.

0195-928X/85/0900-0517$04.50/0

just such a C_p measurement. In this paper, we present a theoretical analysis of these specific heat results, as well as those of Leadbetter [3], Brooks and Bingham [4], and Takahashi [5]. There are several steps in the theoretical analysis that must be completed before the new C_p data can be compared with theory. In fact, the theoretical calculations are carried out for $C_{v_0} \equiv C_{v_0}(V_0, T)$ which represents the specific heat at constant volume reduced to the volume V_0 appropriate for 0 K. In the previous work of Shukla and Plint [1] the reduction from C_p to C_{v_0} was carried out by the Slater–Overton [6, 7] procedure. For aluminum, this procedure, when extended to 900 K, produced an oscillation of the correction term $E(T) = C_v - C_{v_0}$ [in which $C_v \equiv C_v(V, T)$] from positive to negative (500–600 K) and back to positive above 600 K. The anharmonic correction $E(T)$ is small for aluminum and the unphysical oscillation may represent the effects of the approximations of the Slater–Overton procedure and of the uncertainties arising from the assumed thermal expansion and compressibility data. For the alkali metals, which have a much larger anharmonic correction, the Slater–Overton procedure for finding $E(T)$ always produces a positive correction term [8]. To avoid the difficulty mentioned above in Al, we have converted C_v to C_{v_0} by an alternative method using the Murnaghan equation [9]. This procedure yields satisfactory results.

Our earlier theoretical calculation [1] of C_{v_0} was carried out employing the lowest-order (cubic and quartic) anharmonic perturbation theory [$O(\lambda^2)$]. It was not known if the contributions from the higher-order perturbation theory, i.e., of $O(\lambda^4)$, are significant in Al. In this paper, in addition to the λ^2 contributions to C_{v_0}, we calculate the higher-order perturbation (λ^4) contributions to C_{v_0} [10] from an effective Morse potential. From this calculation, we hope to find the relative importance of the λ^2 and λ^4 contributions to C_{v_0}.

A summary of the theoretical calculations, including the λ^4 contributions to C_{v_0} and the reduction of the new experimental data, is presented in Section 2. Here, we note a sharp contrast between the behavior of C_{v_0} for Al determined from the new specific heat data [2] and that shown in Ref. 1, which was based on previous specific heat data [3, 4]. The calculation of the λ^4 contributions to C_{v_0} is also presented in Section 2. The numerical results and discussion are contained in Section 3. The agreement between the theoretical and the new experimental values of $C_{v_0}(T)$ is more than satisfactory in the range 400–900 K. The conclusions of this work are presented in Section 4.

2. REDUCTION OF C_p TO C_{v_0} AND ANHARMONIC CALCULATIONS OF ORDER λ^2 AND λ^4

The correction from C_p to C_{v_0} was made by, first, obtaining the entropy $S_0 = S(V_0, T)$ at the 0 K volume from the experimental entropy $S_v = S(V, T)$ [2] measured at constant pressure p_1 using the relation

$$S_0 = S_v - \int_{V_0}^{V} \left(\frac{\partial p}{\partial T}\right)_V dv \tag{1}$$

The isochores required for the evaluation of the integrand were generated from the Murnaghan equation [9]

$$p_2 - p_1 = \frac{B}{W}\left[\left(\frac{v_1}{v_2}\right)^W - 1\right] \tag{2}$$

in which v_1 and v_2 are the volumes in the states (p_1, T) and (p_2, T), respectively, B is the isothermal bulk modulus in state (p_1, T), and $W = (\partial B/\partial p)_T$ at T. In making the calculations, the isothermal quantities B and W were derived from the corresponding adiabatic quantities B_s and W_s, using the formula

$$1/B = 1/B_s + TV\beta^2/C_p \tag{3}$$

together with the result of Overton [11],

$$W = W_s + Z(1 - 2B'/B\beta - 2W_s) + Z^2(W_s - 1 - \beta'/\beta^2) \tag{4}$$

$$Z = TV\beta^2 B/C_p \tag{5}$$

in which $\beta = (1/V)(\partial V/\partial T)_p$ and the prime denotes differentiation with respect to temperature. (Note that the originally published formulas [11] were in error.)

The data sources used for the quantities β, V, B_s, and W_s were as follows:

β, $V(T < 300)$, Fraser and Hollis-Hallett [12] and Gibbons [13];
β, $V(T > 300)$, Simmons and Balluffi [14];
$B_s(T < 300)$, Kamm and Alers [15];
$B_s(T > 300)$, Gerlich and Fisher [16]; and
W_s, Schmunk and Smith [17].

The isochores were almost straight lines. The slope of each isochore for the temperature range $400 \leqslant T \leqslant 900$ K was obtained by a linear regression. The set of values of $(\partial p/\partial T)_v$ thus found was used to evaluate the integral in Eq. (1) to obtain S_0.

As a second step the electronic contribution [18] to the entropy at the 0 K volume was subtracted. For Al, the coefficient of electronic specific heat, γ, is known from the low-temperature specific heat measurements of Phillips [19]. However, whether one should use this value of γ in the analysis of the high-temperature ($T > \theta_D$) heat capacity and entropy is questionable because of the temperature dependence of the electron–phonon contribution to γ. There are several contributions to γ arising from the free electrons (γ_0), the electron–phonon interaction [$\gamma_1(T)$], the electron–electron interaction (γ_{ee}), and finally, the band structure effects [$\gamma_B(T)$]. The sum total of these contributions to the electronic specific heat C_e is given as

$$C_e = [\gamma_0 + \gamma_1(T) + \gamma_{ee} + \gamma_B(T)]\,T \tag{6}$$

The theoretical calculation of $\gamma_1(T)$ by Grimvall [20] indicates that in the high-temperature limit ($T > \theta_D$), $\gamma_1(T)$ does not contribute. The temperature dependence of $\gamma_B(T)$ is not known in detail at this time. However, we can obtain some estimate of γ_B and γ_{ee} (a small contribution) from the work of Ashcroft and Wilkins [21]. Since the harmonic and anharmonic calculations reported in this paper have been performed in the high-temperature limit, we represent C_e by $(\gamma_0 + \gamma_B)T$ with $\gamma_B = 0.06\gamma_0$ [21], so that $C_e/T = 2.438 \times 10^{-4}$ cal · mol^{-1} · K^{-2}.

The resultant entropy, S_{v_0}, was subjected to a smoothing procedure. Finally, the specific heat at the 0 K volume, $C_{v_0} = T(dS_{v_0}/dT)$, was obtained by four-point differentiation and smoothing of the results.

The difference $\Delta(T) = C_p(T) - C_{v_0}(T)$ between the experimental C_p values and the reduced C_{v_0} for the new data [2] was then subtracted from the literature $C_p(T)$ data [3, 4, 5] to give other sets of C_{v_0} values for comparison purposes. These C_{v_0} values are summarized in Table I. Figure 1 shows the values of C_{v_0} reduced from the new experimental data [2] and the values reduced from literature C_p data [3–5]. The results of the present work show a steadily increasing specific heat (with upward curvature above 550 K) that reaches 3R near 775 K. As found in previous work [1], there is a wide discrepancy in the C_{v_0} values obtained from the C_p results given in Refs. 3 and 4. The Brooks and Bingham data give a C_{v_0} that reaches 3R near 625 K and shows a marked upward curvature for $T > 700$ K. Leadbetter's data give a C_{v_0} that never reaches 3R. The apparent decrease in this C_{v_0} after reaching 5.82 cal · mol^{-1} · K^{-1} at 700 K may be a consequence of errors arising from the end point of the range of specific heat measurements near 750 K. The results from Takahashi's data are similar to those obtained from Leadbetter's data up to 650 K but increase steadily with increasing temperature above 650 K. The graph does

Table I. Values of the Specific Heat at 0 K Volume Reduced from the Experimental Data of Four Investigations

	C_{v_0} (cal · mol^{-1} · K^{-1})			
T (K)	New results, Ref. 2	Ref. 3	Ref. 4	Ref. 5
400	5.665	5.598	5.664	5.580
450	5.735	5.655	5.752	5.648
500	5.780	5.732	5.814	5.703
550	5.814	5.762	5.868	5.756
600	5.839	5.798	5.922	5.794
650	5.870	5.814	5.979	5.815
700	5.900	5.824	6.052	5.826
750	5.936	5.798	6.123	5.866
800	5.974		6.206	5.904
850	6.013		6.320	5.931
900	6.060			

not reach 3R by 850 K. The C_{v_0} curve from Takahashi's data is essentially parallel to that obtained from the new data but is consistently lower over the entire temperature range shown in Fig. 1.

For any of these curves the portion above 3R must be accounted for by invoking the anharmonic and vacancy contributions to C_{v_0}. To separate these two contributions we need to calculate *all* the anharmonic contributions to C_{v_0}, and then the remainder must be the vacancy contribution because there are no other excitations in Al which contribute to C_{v_0} in the temperature range 700–950 K.

First, let us examine the anharmonic effect. This can be evaluated either by the lattice dynamics method [i.e., the perturbation theory (PT) or the self-consistent phonon theory], which is valid for all temperatures, or by computer simulation techniques such as the Monte Carlo and molecular dynamics methods, which are usually applicable in the classical high-temperature limit ($T > \theta_D$, where θ_D is the Debye temperature). Among these methods only the perturbation method has been applied up to now in the calculation of C_{v_0} for Al by Shukla and Plint [1]. Their calculation was carried out employing the lowest-order perturbation theory, which requires the numerical evaluation of *two* terms in the Helmholtz function (F). These terms arise from the cubic and quartic terms of the Taylor expansion of the crystal potential energy [$V(r)$].

If we denote the perturbation expansion parameter by λ, defined as the ratio of a typical root mean square atomic displacement and the nearest-

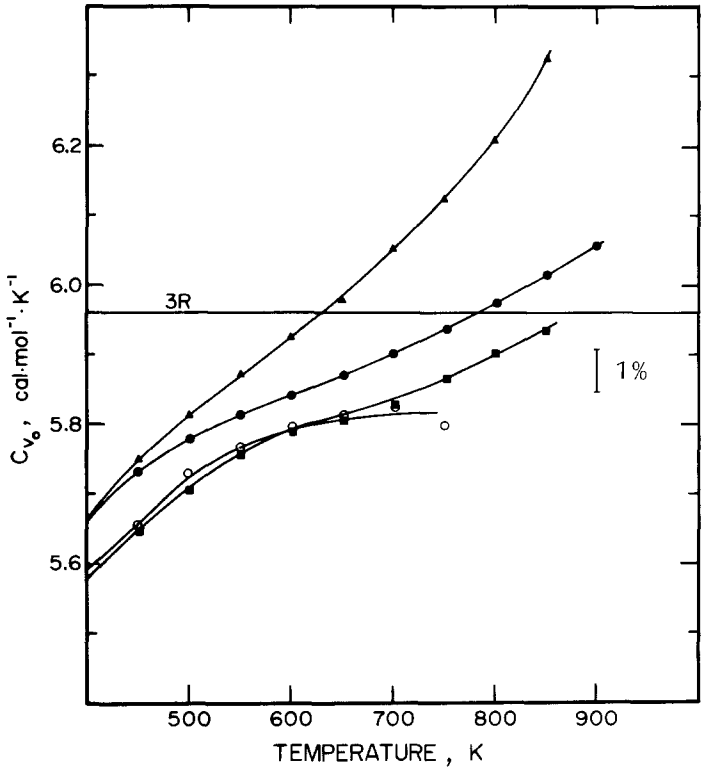

Fig. 1. Reduced specific heat of Al at 0 K volume (C_{v_0}) versus temperature (T). (▲) From smoothed data of Brooks and Bingham [4]; (●) from smoothed new data [2]; (■) from smoothed data of Takahashi [5]; (○) from smoothed data of Leadbetter [3]. The bar at the right represents 1% of 3R.

neighbor distance, the lowest-order PT contributions to F are of $O(\lambda^2)$ and their contribution to C_{v_0} is proportional to T in the high-temperature limit. Since our "experimental" C_{v_0} indicates an upward curvature, it is necessary to look for additional anharmonic contributions to C_{v_0} which vary as T^2. In fact it has been shown by Shukla and Cowley [10] that *all* the T^2 contributions are given by the PT of $O(\lambda^4)$, which requires the numerical evaluation of *eight* terms in F. The anharmonic Hamiltonian (H_A) is given by

$$H_A = \lambda V_3 + \lambda^2 V_4 + \lambda^3 V_5 + \lambda^4 V_6 \tag{7}$$

which is obtained by expanding the potential energy in powers of the atomic displacement and truncating the expansion after the sixth-degree term. The eight contributions to F of $O(\lambda^4)$ arise from the V_6, V_4–V_4,

V_3–V_5, V_3–V_3–V_4, and V_3–V_3–V_3–V_3 interactions in the first-, second-, third-, and fourth-order perturbation theory, respectively. In the diagrammatic language, these contributions to F have been derived by Shukla and Cowley [10]. It should be noted that there are two distinct contributions or diagrams for each of the V_4–V_4, V_3–V_3–V_4, and V_3–V_3–V_3–V_3 interactions, whereas there is only one distinct diagram for the V_6 and V_3–V_5 interactions. We present these diagrams and the two lowest-order λ^2 diagrams in Figs. 3 and 2, respectively. Symbolically they represent the various phonon lines connecting the different vertices V_n ($n = 1, 2, ..., 6$) for the different combinations listed above. In the high-temperature limit, their contributions to F are listed in Table II, where the meaning of the various symbols is as follows: $\hbar$ is Planck's constant divided by 2π, $\beta = (k_B T)^{-1}$, k_B is the Boltzmann constant, $\omega(\lambda_k)$ is the phonon frequency for the mode $\lambda_k = (\vec{q}_k j_k)$, $\vec{q}_k$ is the wave vector, and j_k is the branch index. In general the V function is defined by

$$V(\lambda_1, ..., \lambda_n) = \left(\frac{1}{n!}\right) N^{1-n/2} \Delta(\vec{q}_1 + \cdots + \vec{q}_n) \times \left(\frac{\hbar}{2^n \omega(\lambda_1) \cdots \omega(\lambda_n)}\right)^{1/2} \Phi(\lambda_1, ..., \lambda_n) \tag{8}$$

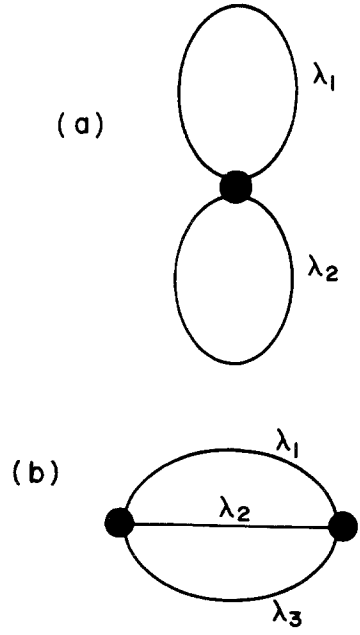

Fig. 2. Diagrams of order λ^2 (cf. text).

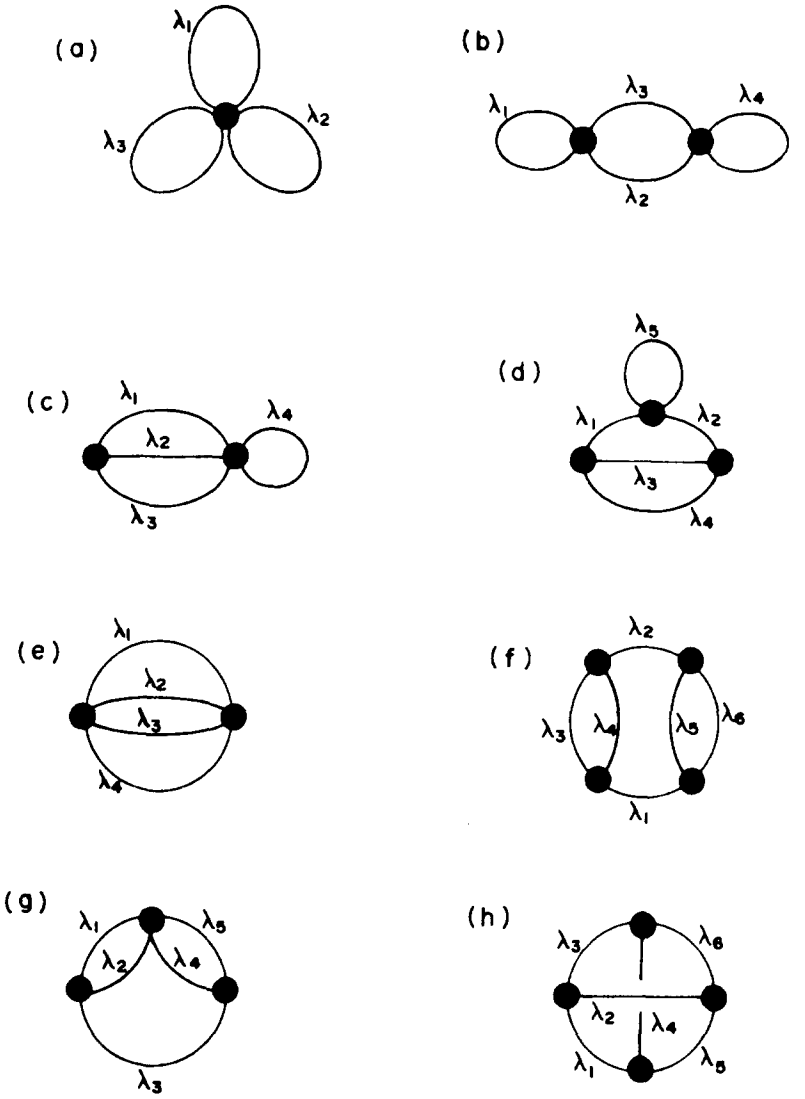

Fig. 3. Diagrams of order λ^4 (cf. text).

Table II. High-Temperature Limits for the Various Contributions to the Free Energy Given by Shukla and Cowley [10]

Fig. No.	High-temperature limit
2a	$\left(\frac{3}{\beta^2}\right)\left(\frac{2}{\hbar}\right)^2 \sum_{\lambda_1,\lambda_2} \frac{V(\lambda_1, -\lambda_1, \lambda_2, -\lambda_2)}{\omega(\lambda_1)\,\omega(\lambda_2)}$
2b	$-\frac{3}{\beta^2}\left(\frac{2}{\hbar}\right)^3 \sum_{\lambda_1,\lambda_2,\lambda_3} \frac{\lvert V(\lambda_1, \lambda_2, \lambda_3)\rvert^2}{\omega(\lambda_1)\,\omega(\lambda_2)\,\omega(\lambda_3)}$
3a	$\frac{15}{\beta^3}\left(\frac{2}{\hbar}\right)^3 \sum_{\lambda_1,\lambda_2,\lambda_3} \frac{V(\lambda_1, -\lambda_1, \lambda_2, -\lambda_2, \lambda_3, -\lambda_3)}{\omega(\lambda_1)\,\omega(\lambda_2)\,\omega(\lambda_3)}$
3b	$-\frac{36}{\beta^3}\left(\frac{2}{\hbar}\right)^4 \sum_{\lambda_1,\lambda_2,\lambda_3,\lambda_4} \frac{V(\lambda_1, -\lambda_1, \lambda_2, \lambda_3)\,V(-\lambda_2, -\lambda_3, \lambda_4, -\lambda_4)}{\omega(\lambda_1)\,\omega(\lambda_2)\,\omega(\lambda_3)\,\omega(\lambda_4)}$
3c	$-\frac{60}{\beta^2}\left(\frac{2}{\hbar}\right)^4 \sum_{\lambda_1,\lambda_2,\lambda_3,\lambda_4} \frac{V(\lambda_1, \lambda_2, \lambda_3)\,V(-\lambda_1, -\lambda_2, -\lambda_3, \lambda_4, -\lambda_4)}{\omega(\lambda_1)\,\omega(\lambda_2)\,\omega(\lambda_3)\,\omega(\lambda_4)}$
3d	$\frac{108}{\beta^3}\left(\frac{2}{\hbar}\right)^5 \sum_{\lambda_1,\lambda_2,\lambda_3,\lambda_4,\lambda_5} \frac{V(\lambda_1, \lambda_3, \lambda_4)\,V(-\lambda_2, -\lambda_3, -\lambda_4)\,V(-\lambda_1, \lambda_2, \lambda_5, -\lambda_5)}{\omega(\lambda_1)\,\omega(\lambda_2)\,\omega(\lambda_3)\,\omega(\lambda_4)\,\omega(\lambda_5)}$
3e	$-\frac{12}{\beta^3}\left(\frac{2}{\hbar}\right)^4 \sum_{\lambda_1,\lambda_2,\lambda_3,\lambda_4} \frac{\lvert V(\lambda_1, \lambda_2, \lambda_3, \lambda_4)\rvert^2}{\omega(\lambda_1)\,\omega(\lambda_2)\,\omega(\lambda_3)\,\omega(\lambda_4)}$
3f	$-\frac{81}{\beta^3}\left(\frac{2}{\hbar}\right)^6 \sum_{\lambda_1,\lambda_2,\lambda_3,\lambda_4,\lambda_5,\lambda_6} \frac{V(\lambda_1, \lambda_3, \lambda_4)\,V(-\lambda_1, \lambda_5, \lambda_6)\,V(\lambda_2, -\lambda_3, -\lambda_4)\,V(-\lambda_2, -\lambda_5, -\lambda_6)}{\omega(\lambda_1)\,\omega(\lambda_2)\,\omega(\lambda_3)\,\omega(\lambda_4)\,\omega(\lambda_5)\,\omega(\lambda_6)}$
3g	$\frac{108}{\beta^3}\left(\frac{2}{\hbar}\right)^5 \sum_{\lambda_1,\lambda_2,\lambda_3,\lambda_4,\lambda_5} \frac{V(\lambda_1, \lambda_2, \lambda_4, \lambda_5)\;V(-\lambda_1, -\lambda_2, \lambda_3)\,V(-\lambda_3, -\lambda_4, -\lambda_5)}{\omega(\lambda_1)\,\omega(\lambda_2)\,\omega(\lambda_3)\,\omega(\lambda_4)\,\omega(\lambda_5)}$
3h	$-\frac{54}{\beta^3}\left(\frac{2}{\hbar}\right)^6 \sum_{\lambda_1,\lambda_2,\lambda_3,\lambda_4,\lambda_5,\lambda_6} \frac{V(\lambda_1, \lambda_2, \lambda_3)\,V(-\lambda_1, \lambda_4, \lambda_5)\,V(-\lambda_2, -\lambda_5, \lambda_6)\,V(-\lambda_3, -\lambda_4, -\lambda_6)}{\omega(\lambda_1)\,\omega(\lambda_2)\,\omega(\lambda_3)\,\omega(\lambda_4)\,\omega(\lambda_5)\,\omega(\lambda_6)}$

where N denotes the number of unit cells in the crystal and $\Delta(\vec{q}_1+\vec{q}_2+\cdots\vec{q}_n)=1$ if the argument of the Δ function is a vector of the reciprocal lattice (including zero) and zero otherwise. The Φ function is defined by

$$\Phi(\lambda_1,\ldots,\lambda_n)=\frac{1}{2M^{n/2}}\sum_{l}{}'\sum_{\alpha\beta\cdots\gamma}\phi_{\alpha\beta\cdots\gamma}(|\vec{R}_l|)\,e_\alpha(\lambda_1)\,e_\beta(\lambda_2)\cdots e_\gamma(\lambda_n)$$
$$\times\prod_{j=1}^{n}[1-\exp(i\vec{q}_j\cdot\vec{R}_l)] \tag{9}$$

where M is the atomic mass, $\vec{R}_l$ is a vector of the direct lattice, and $e_\alpha(\lambda_j)$ $(j=1,\ldots,n)$ are the components of the eigen-vector $\vec{e}(\lambda_j)$. The prime over the l summation indicates the omission of the origin point.

The calculation of the diagrams presented in Fig. 3 is extremely complicated because of the multiple Brillouin zone (BZ) sums as well as the summation over the neighbors and the tensors $\phi_{\alpha\beta\cdots\gamma}$. So far, they have been evaluated only for the Lennard–Jones nearest-neighbor interaction potential for the fcc crystal by Shukla and Cowley [10] and Shukla and Wilk [22]. To get some idea of the magnitude of F to $O(\lambda^4)$ in Al, here we have chosen to calculate the above eight contributions for the Morse potential. Recently the nearest-neighbor interaction Morse potential has been used successfully in the calculation of the thermal expansion and other thermodynamic properties by Shukla and MacDonald [23] and MacDonald and MacDonald [24]. The Morse potential with its parameters D, α, and r_0 for Al is given in Ref. 23:

$$\phi(r)=D\{\exp[-2\alpha(r-r_0)-2\exp[-\alpha(r-r_0)]\} \tag{10}$$

where $D=0.6369\times10^{-12}$ erg, $\alpha=1.1611\ (\text{Å})^{-1}$, and $r_0=2.8485$ Å.

The tensors $\phi_{\alpha\beta\cdots\gamma}$ needed in the calculation of the diagrams of $O(\lambda^2)$ and $O(\lambda^4)$ are obtained by differentiating the above potential. The $\omega(\vec{q}j)$ and $\vec{e}(\vec{q}j)$ are obtained by diagonalizing the dynamical matrix $D_{\alpha\beta}(\vec{q})$, which satisfies the eigenvalue equation

$$\sum_{\beta}D_{\alpha\beta}(\vec{q})\,e_\beta(\vec{q}j)=\omega^2(\vec{q}j)\,e_\alpha(\vec{q}j) \tag{11}$$

where $D_{\alpha\beta}(\vec{q})$ is obtained from the second-rank tensor derived from the Morse potential.

The closed loops appearing in Figs. 2a and 3a–d involve a single BZ sum which has been evaluated with 108,000 points in the whole zone. The other diagrams (Figs. 2b and 3c, d, and f), in which the phonon lines connect the different vertices, have been evaluated with 500 wave vectors in the

whole zone. We have used a combination of 215 odd and even wave vectors in the calculation of Figs. 3g and h, and finally, Fig. 3e has been evaluated by the plane-wave method as given by Shukla and Wilk [22]. We omit the rest of the details of the calculation of the diagrams, as they are given by Shukla and Wilk [22].

The harmonic contribution to C_{v_0} is calculated from the well-known formula

$$C_{v_0}^h = k_B \sum_{\vec{q}j} \left[\frac{\hbar\omega(\vec{q}j)}{2k_B T}\right]^2 \text{Cosech}^2\left(\frac{\hbar\omega(\vec{q}j)}{k_B T}\right) \tag{12}$$

In the work of Shukla and Plint [1], the above expression was evaluated numerically by performing the $\vec{q}j$ summations for a large number of points in the Brillouin zone. It was noted by Shukla and Plint that the three-term high-temperature expansion gave the same results as Eq. (12) in the temperature range 550–900 K. In the present work, we are able to evaluate this expression analytically for the central-force nearest-neighbor model of the fcc crystal. The high-temperature $\{[\hbar\omega(\vec{q}j)/2k_B T] < 1\}$ three-term expansion of $C_{v_0}^h$ is

$$C_{v_0}^h = k_B \sum_{\vec{q}j} \left\{1 - \frac{1}{3}\left[\frac{\hbar\omega(\vec{q}j)}{2k_B T}\right]^2 + \frac{1}{15}\left[\frac{\hbar\omega(\vec{q}j)}{2k_B T}\right]^4 + \cdots\right\} \tag{13}$$

The sums $\sum_{\vec{q}j} \omega^2(\vec{q}j)$ and $\sum_{\vec{q}j} \omega^4(\vec{q}j)$ can be evaluated from the eigenvalue equation (Eq. 11). Omitting the details we find the following:

$$C_{v_0}^h = 3Nk_B\left[1 - \frac{1}{3M}\left(\frac{\hbar}{k_B T}\right)^2\left(\phi'' + \frac{2}{r}\phi'\right) + \frac{1}{12M^2}\left(\frac{\hbar}{k_B T}\right)^4\left(\phi'' + \frac{2}{r}\phi'\right)^2\right] \tag{14}$$

where ϕ' and ϕ'', the first and second derivatives of $\phi(r)$, are evaluated from Eq. (10).

3. RESULTS AND DISCUSSION

The numerical results for all the diagrams of $O(\lambda^2)$ and $O(\lambda^4)$ for the nearest-neighbor Morse potential are presented in Table III. It is interesting to note that among the λ^4 diagrams, the contribution from Fig. 3b is close to that of the total $F(\lambda^4)$. In fact the sum of Figs. 3a and b is only 2.5% lower than the total $F(\lambda^4)$.

A detailed calculation of the harmonic and anharmonic (λ^2) values for C_{v_0} indicates that although the contribution to C_{v_0} from $F(\lambda^4)$ is three times larger than that from $F(\lambda^2)$, it is not sufficient to account for the upward

Table III. Anharmonic Contributions to the Helmholtz Free Energy (Figs. 2a and b) are in Units of $N(k_B T)^2 \times 10^{12}\,\mathrm{erg}^{-1}$ and Figs. 3a–h are in Units of $N(k_B T)^3 \times 10^{24}\,\mathrm{erg}^{-2}$)

Fig. No.	Contribution
F(2a)	0.38012
F(2b)	−0.40767
Total $F(\lambda^2) = -0.02755\ N(k_B T)^2 \times 10^{12}\,\mathrm{erg}^{-1}$	
F(3a)	0.01742
F(3b)	−0.21506
F(3c)	−0.38556
F(3d)	0.60435
F(3e)	−0.34431
F(3f)	−0.50573
F(3g)	0.74463
F(3h)	−0.11823
Total $F(\lambda^4) = -0.20249\ N(k_B T)^3 \times 10^{24}\,\mathrm{erg}^{-2}$	

curvature in C_{v_0}. The total contribution (λ^2 and λ^4) from the Morse potential [23] is very similar to that from two of the pseudopotentials (Ashcroft [27] and Harrison point ion [26]).

We present in Table IV and Fig. 4 the values of the total C_{v_0}, harmonic plus anharmonic, to $O(\lambda^2)$, calculated for the three pseudopotentials used in Ref. 1 (curves 1–3) and for the Morse potential, with the anharmonic contribution to $O(\lambda^2)$ (curve 4) and to $O(\lambda^4)$ (also curve 2). Only the DRT potential [28] gives a C_{v_0} that rises above 3R, while, at best, the Harrison and Morse [to $O(\lambda^4)$] potentials give a C_{v_0} that approaches 3R at 900 K.

From the results presented in Table IV, it is interesting to see that the results for C_{v_0} obtained from the nearest-neighbor (harmonic as well as anharmonic) Morse potential are so close to the Ashcroft (a sixth-neighbor harmonic and anharmonic interaction) and Harrison point ion (13-neighbor harmonic and 8-neighbor anharmonic interaction) pseudopotentials. The latter two potentials have a much more sound theoretical basis than the Morse potential and involve a large number of neighbors in the harmonic and anharmonic calculations.

In Fig. 4 we also present the reduced C_{v_0} values obtained from the new experimental data [2]. They lie on a smooth curve (curve 5) which exhibits an upward curvature for $T > 550$ K and rises above 3R near 800 K. Since

Table IV. Total Calculated Harmonic Plus Anharmonic Contributions to the Constant-Volume (0 K) Specific Heat of Aluminum for Three Pseudopotentials and One Phenomenological Potential

T (K)	C_{v_0} (cal · mol^{-1} · K^{-1})				
	Harrison [26]	Ashcroft [27]	DRT [28]	Morse (λ^2)	Morse ($\lambda^2+\lambda^4$) [23]
400	5.68707	5.70620	5.73119	5.69960	5.70757
450	5.75109	5.75849	5.79524	5.75499	5.76507
500	5.79842	5.80303	5.84347	5.79536	5.80781
550	5.83460	5.83689	5.88116	5.82570	5.84076
600	5.86307	5.86349	5.91155	5.84912	5.86704
650	5.88605	5.88483	5.93676	5.86761	5.88865
700	5.90500	5.90237	5.95818	5.88250	5.90690
750	5.92095	5.91704	5.97676	5.89470	5.92271
800	5.93461	5.92956	5.99317	5.90484	5.93670
850	5.94649	5.94042	6.00792	5.91340	5.94938
900	5.95697	5.94990	6.02134	5.92070	5.96103

none of the calculated curves shows any upward curvature, we have corrected the experimental C_{v_0} for a vacancy contribution C_v^{vac} using the expression

$$C_v^{\text{vac}} = (Nk_B)\exp(\Delta S/k_B)(E/k_B T)^2 \exp[-(E/k_B T)] \tag{15}$$

where E and ΔS are the energy and entropy of formation of a single vacancy, respectively. We use $E = 0.66$ eV [25] and estimate that $(\Delta S/k_B) \leqslant 1.8$ on the ground that the corrected $C_{v_0} - C_v^{\text{vac}}$ should not exhibit a negative temperature derivative. Curve 6 in Fig. 4 was obtained with $(\Delta S/k_B) = 1.4$. The vacancy contribution is evident at 600 K. The agreement between this curve and the calculated values shown in curves 2 and 3 is very satisfactory. While curve 6 lies below curves 2 and 3 over the entire temperature range $500 \leqslant T \leqslant 900$ K, the difference between them is only about 0.5%. After correction for vacancies, the experimental C_{v_0} does not reach 3R by 900 K.

It should be noted that variation of the quantity W, Eq. (4), by 10%, to allow for experimental uncertainty in its value, makes a change of less than 0.2% in the reduced values of C_{v_0}.

A comparison of the sets of values of the reduced C_{v_0} derived from previous experimental data [3–5] with the present values calculated from perturbation theory does not alter our previous conclusions [1]. The

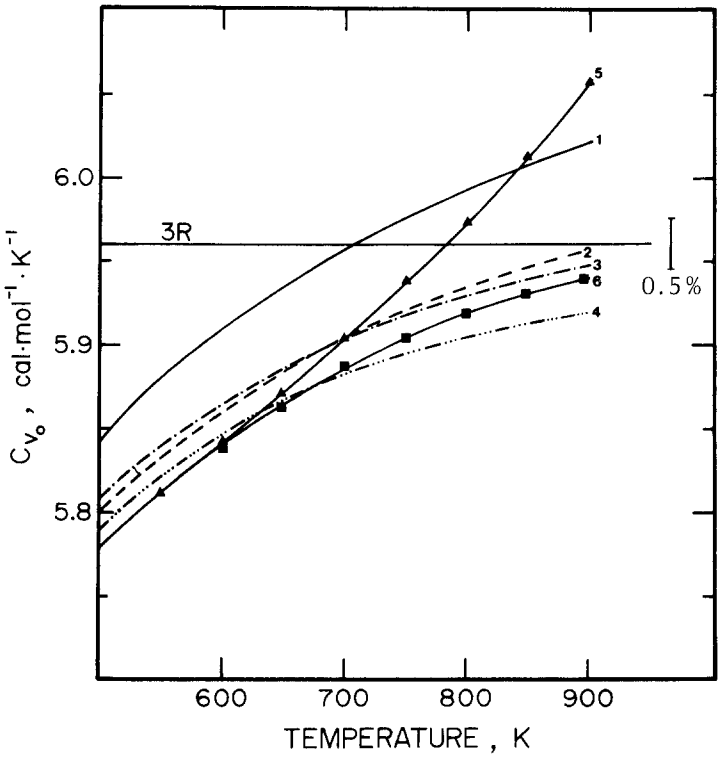

Fig. 4. Calculated specific heat of Al at 0 K volume (C_{v_0}) versus temperature (T) for four potentials (curves 1–4) and reduced specific heat for two sets of new experimental data (curves 5 and 6). Curve 1 (——), from Dagens et al. potential [28]; curve 2 (– – –) from Harrison modified point ion potential [26]; curve 3 (— · —), from Ashcroft potential [27]; curve 4 (— · · · —), from effective Morse potential [23] to $O(\lambda^2)$; curve 5 (▲), from smoothed new data [2]; curve 6 (■), curve 5 data corrected for the vacancy contribution to the specific heat. The effective Morse potential to $O(\lambda^4)$ gives results that are indistinguishable from curve 2 on the scale of this figure. The bar at the right represents 0.5% of 3R.

results of Leadbetter [3] and of Takahashi [5] still yield values of C_{v_0} that fall below the lowest of the calculated curves, even without correction for vacancy effects above 600 K. The results of Brooks and Bingham [4] still yield values that lie well above the DRT curve for most of the temperature range, and a reasonable vacancy correction still does not bring about significantly improved agreement with any of the calculated curves. As noted earlier, the $O(\lambda^4)$ contribution to C_{v_0} is greater than the $O(\lambda^2)$ contribution, thereby implying the need for a summation of all the con-

tributions from the perturbation series. It is unlikely that the total contribution evaluated by this procedure will produce a substantial rise in C_{v_0} that will match the upward curvature.

4. CONCLUSION

The new C_p data for Al reported in the preceding paper [2] has been reduced to C_{v_0} using the Murnaghan equation. The lowest-order anharmonic contributions are evaluated from a nearest-neighbor phenomenological Morse potential and several pseudopotentials. The contributions of the higher-order perturbation theory anharmonic terms to C_{v_0} are evaluated for the nearest-neighbor Morse potential. It is concluded that the vacancy contributions to C_{v_0} are more important than the higher-order anharmonic terms. After removal of the vacancy contribution from the values of C_{v_0} obtained from the new C_p data, excellent agreement is achieved between the theory and the experiment. It is also shown that the Morse potential results for C_{v_0} are just about the same as those from the more sophisticated Ashcroft and Harrison modified point ion pseudopotentials.

ACKNOWLEDGMENTS

The new experimental research which the present work interprets was supported in part by the U.S. Air Force Office of Scientific Research. R. C. Shukla acknowledges the support of the Natural Sciences and Engineering Research Council of Canada.

REFERENCES

1. R. C. Shukla and C. A. Plint, *Int. J. Thermophys.* **1**:299 (1980).
2. D. A. Ditmars, C. A. Plint, and R. C. Shukla, *Int. J. Thermophys.* **6**:499 (1985).
3. A. J. Leadbetter, *J. Phys. C (Proc. Phys. Soc.)* **1**:1481 (1968).
4. C. R. Brooks and R. E. Bingham, *J. Phys. Chem. Solids* **29**:1553 (1968).
5. Y. Takahashi, Private communication, 4 Dec. 1981.
6. J. C. Slater, *Introduction to Chemical Physics* (McGraw–Hill, New York, 1939), Chap. XIII.
7. W. C. Overton, *J. Chem. Phys.* **37**:2975 (1962).
8. R. C. Shukla and C. A. Plint, in *Proceedings of the Eighth Symposium on Thermophysical Properties of Solids and of Selected Fluids for Energy Technology*, J. V. Sengers, ed. (ASME, New York, 1982), p. 77.
9. F. D. Murnaghan, *Proc. Natl. Acad. Sci.* **30**:244 (1944).
10. R. C. Shukla and E. R. Cowley, *Phys. Rev.* **B3**:4055 (1971).
11. W. C. Overton, *J. Chem. Phys.* **37**:116 (1962).
12. D. B. Fraser and A. C. Hollis-Hallett, *Can. J. Phys.* **43**:193 (1965).

13. D. F. Gibbons, *Phys. Rev.* **112**:136 (1958).
14. R. O. Simmons and R. W. Balluffi, *Phys. Rev.* **117**:52 (1960).
15. G. N. Kamm and G. A. Alers, *J. Appl. Phys.* **35**:327 (1964).
16. D. Gerlich and E. S. Fisher, *J. Phys. Chem. Solids* **30**:1197 (1969).
17. R. E. Schmunk and C. S. Smith, *J. Phys. Chem. Solids* **9**:100 (1959).
18. A. J. Leadbetter, *J. Phys. C (Proc. Phys. Soc.)* **1**:1489 (1968).
19. N. E. Phillips, *Phys. Rev.* **114**:676 (1959).
20. G. Grimvall, *J. Phys. Chem. Solids* **29**:1221 (1968).
21. N. W. Ashcroft and J. W. Wilkins, *Phys. Lett.* **14**:285 (1965).
22. R. C. Shukla and L. Wilk, *Phys. Rev.* **B10**:3660 (1974).
23. R. C. Shukla and R. A. MacDonald, *High Temp. High Press.* **12**:291 (1980).
24. R. A. MacDonald and W. M. MacDonald, *Phys. Rev.* **B24**:1715 (1981).
25. W. Triftshäuser, *Phys. Rev.* **B12**:4634 (1975).
26. W. A. Harrison, *Pseudopotentials in the Theory of Metals* (Benjamin, New York, 1966).
27. N. W. Ashcroft, *Phys. Lett.* **23**:48 (1966).
28. L. Dagens, M. Rasolt, and R. Taylor, *Phys. Rev.* **B11**:2726 (1975).